Molecules and Cells

CHIP and BAP1 Act in Concert to Regulate INO80 Ubiquitination and Stability for DNA Replication

Hye-Ran Seo[1,2], Daun Jeong[1,2], Sunmi Lee[1], Han-Sae Lee[1,2], Shin-Ai Lee[1,2,3], Sang Won Kang[1], and Jongbum Kwon[1,2,*]

[1]Department of Life Science, Ewha Womans University, Seoul 03760, Korea, [2]The Research Center for Cellular Homeostasis, Ewha Womans University, Seoul 03760, Korea, [3]Present address: Laboratory of Genitourinary Cancer Pathogenesis, Center for Cancer Research, National Cancer Institute, Bethesda, MD 20892, USA
*Correspondence: jongkwon@ewha.ac.kr
https://doi.org/10.14348/molcells.2021.2258
www.molcells.org

The INO80 chromatin remodeling complex has roles in many essential cellular processes, including DNA replication. However, the mechanisms that regulate INO80 in these processes remain largely unknown. We previously reported that the stability of Ino80, the catalytic ATPase subunit of INO80, is regulated by the ubiquitin proteasome system and that BRCA1-associated protein-1 (BAP1), a nuclear deubiquitinase with tumor suppressor activity, stabilizes Ino80 via deubiquitination and promotes replication fork progression. However, the E3 ubiquitin ligase that targets Ino80 for proteasomal degradation was unknown. Here, we identified the C-terminus of Hsp70-interacting protein (CHIP), the E3 ubiquitin ligase that functions in cooperation with Hsp70, as an Ino80-interacting protein. CHIP polyubiquitinates Ino80 in a manner dependent on Hsp70. Contrary to our expectation that CHIP degrades Ino80, CHIP instead stabilizes Ino80 by extending its half-life. The data suggest that CHIP stabilizes Ino80 by inhibiting degradative ubiquitination. We also show that CHIP works together with BAP1 to enhance the stabilization of Ino80, leading to its chromatin binding. Interestingly, both depletion and overexpression of CHIP compromise replication fork progression with little effect on fork stalling, as similarly observed for BAP1 and Ino80, indicating that an optimal cellular level of Ino80 is important for replication fork speed but not for replication stress suppression. This work therefore idenitifes CHIP as an E3 ubiquitin ligase that stabilizes Ino80 via nondegradative ubiquitination and suggests that CHIP and BAP1 act in concert to regulate Ino80 ubiquitination to fine-tune its stability for efficient DNA replication.

Keywords: BRCA1-associated protein 1, C-terminus of Hsp70-interacting protein, DNA replication, INO80 chromatin remodeler, ubiquitin

INTRODUCTION

The INO80 complex is a member of the ATP-dependent chromatin remodeling complex family and consists of more than 10 subunits, including Ino80—the catalytic ATPase subunit that is an integral component of the complex and is responsible for chromatin remodeling activity—as well as the associated proteins that play regulatory roles (Jin et al., 2005; Shen et al., 2000). Similar to other chromatin remodelers, INO80 functions in transcriptional regulation of a subset of cellular genes (Conaway and Conaway, 2009; Morrison and Shen, 2009; Shen et al., 2003). A notable feature of INO80 is its direct involvement in a variety of nontranscriptional nuclear events, including replication fork progression, stress-induced stalled fork recovery (Hur et al., 2010; Lee et al., 2014; 2019; Papamichos-Chronakis and Peterson, 2008; Shimada et al.,

Received 28 December, 2020; revised 9 February, 2021; accepted 14 February, 2021; published online 25 February, 2021

eISSN: 0219-1032
©The Korean Society for Molecular and Cellular Biology. All rights reserved.
This is an open-access article distributed under the terms of the Creative Commons Attribution-NonCommercial-ShareAlike 3.0 Unported License. To view a copy of this license, visit http://creativecommons.org/licenses/by-nc-sa/3.0/.

2008; Vassileva et al., 2014; Vincent et al., 2008), DNA damage repair and checkpoint responses (Downs et al., 2004; Morrison et al., 2004; 2007; Papamichos-Chronakis et al., 2006; Park et al., 2010; Tsukuda et al., 2005), telomere replication and telomere length regulation (Min et al., 2013; Yu et al., 2007), centromere stability, spindle assembly and chromosome segregation (Measday et al., 2005; Ogiwara et al., 2007; Park et al., 2011).

Consistent with the role of INO80 in chromosomal processes crucial for genome integrity, depletion of INO80 causes aneuploidy and chromosome structural abnormalities, which may potentially lead to the development of diseases, such as cancer (Chambers et al., 2012; Hur et al., 2010; Papamichos-Chronakis et al., 2011; Wu et al., 2007). Emerging evidence suggests that INO80 is associated with tumorigenesis. The tumor suppressor BRCA1-associated protein-1 (BAP1) stabilizes Ino80 via deubiquitination, thereby ensuring DNA replication and genome integrity (Lee et al., 2014). Ino80 is downregulated in BAP1-defective mesothelioma, owing to the lack of a BAP1-mediated Ino80 stabilization mechanism, thus raising the possibility of a tumorigenic role for INO80 in this cancer (Lee et al., 2014). In addition, Ino80 haploinsufficiency shifts the tumor type from lymphoma to sarcoma in mice on a p53-null background, probably as a result of increased genomic instability (Min et al., 2013). However, recent reports have demonstrated that INO80 acts oncogenically in tumorigenesis in several human cancers, such as melanoma, and colon, cervical and non-small cell lung cancers (Hu et al., 2016; Lee et al., 2017; Zhang et al., 2017; Zhou et al., 2016).

The carboxyl terminus of Hsp70-interacting protein (CHIP, also called STUB1) is a specialized U box-containing E3 ligase that functions together with protein chaperones, such as Hsp70 and Hsp90 (Hatakeyama et al., 2001; Jiang et al., 2001; Murata et al., 2001). CHIP has three tandem tetratricopeptide repeat (TPR) motifs through which it interacts with chaperones and ubiquitinates chaperone-bound substrates. Thus, CHIP serves as a molecular link between cellular protein folding and degradation by functioning as both a cochaperone and an E3 ubiquitin ligase (Connell et al., 2001; Hohfeld et al., 2001). CHIP plays a critical role in a wide range of biological functions by targeting various protein substrates, including those associated with tumorigenesis (Seo et al., 2019; Wang et al., 2020).

Although chromatin remodelers, including INO80, play critical roles in many essential biological processes, little is known about the mechanisms that regulate their protein stability. Our previous study reported Ino80 as the first identified chromatin remodeler regulated by the ubiquitin-proteasome degradation pathway and identified BAP1 as a deubiquitinase for Ino80. Following up on this study, we initiated the present investigation to identify the E3 ubiquitin ligase that targets Ino80 for proteasomal degradation. We identified CHIP as an E3 ligase that interacts with and polyubiquitinates Ino80 in an Hsp70-dependent manner. Contrary to our expectation, CHIP stabilized Ino80 rather than leading to its degradation. We provide evidence that CHIP stabilizes Ino80 by inhibiting its degradative ubiquitination and works together with BAP1 to regulate the ubiquitination and stability of Ino80 for efficient DNA replication.

MATERIALS AND METHODS

Cells and antibodies

HEK 293T human embryonic kidney and HT29 human colon cancer cells were purchased from ATCC (USA), and cultured in Dulbecco's Modified Eagle's Medium (12800-082; Gibco, USA) and McCOY's 5A modified medium, respectively, supplemented with 10% fetal bovine serum (HyClone, USA), 100 U/ml penicillin and 100 μg/ml streptomycin. The sources of the primary antibodies were as follows: anti-Actin (sc-8432; Santa Cruz Biotechnology, USA), anti-α-tubulin (ab18251; Abcam, UK), anti-BAP1 (sc-28383; Santa Cruz Biotechnology), anti-CHIP (2080; Cell Signaling Technology, USA), anti-Flag (F3165 and F7425; Sigma, USA), anti-GAPDH (LF-PA0212; AbFrontier, Korea), anti-H2A (07-146; Millipore, USA), anti-Ha (sc-7392; Santa Cruz Biotechnology), anti-Hsp70 (sc-32239; Santa Cruz Biotechnology), anti-Ino80 (ab105451 and Bethyl, A303-371A; Abcam), anti-Myc (sc-789 and sc-40; Santa Cruz Biotechnology).

Plasmid vectors, siRNAs and transfection

The plasmid vectors for Flag-Ino80-Δ4 to Flag-Ino80-Δ9 were constructed by cloning polymerase chain reaction products from Flag-Ino80 into the Not1-EcoRV sites of 3xFlag-CMV vector using the following primers: forward primers, Ino80-Δ4, 5′-gct ggc ggc cgc atg cag aga tac ctg agg aac aag; Ino80-Δ5, 5′-gct ggc ggc cgc atg gca gaa tat gaa agg cga gtt; Ino80-Δ6, 5′-gct ggc ggc cgc atg ctt atc tac tcc cag atg acc; Ino80-Δ7, 5′-gct ggc ggc cgc atg cac cgc tta ggg cag aca aag; Ino80-Δ8, 5′-gct ggc ggc cgc atg cgg atg gtg att tca ggt ggg; Ino80-Δ9, 5′-gct ggc ggc cgc atg cgg cag gaa gag aaa cgg caa, and reverse primers, 5′-gcc gga tat cag ccg tcc tcc aga ggg gtt. The vectors for Flag-Ino80-Δ1, -Δ2, -Δ3 and -Δ10 were as previously described (Lee et al., 2014; Park et al., 2011). The expression vectors for Myc-CHIP and Myc-CHIP-ΔUbox were as previously described (Oh et al., 2011). The BAP1 and BAP1(C91S) expression vectors were previously described (Lee et al., 2014). All plasmid transfections were performed with PEI (polyethylenimine, branched; 408727; Sigma). The sequences of siRNA are as follows: si-Ino80, 5′-uua aga gug uga uuu cuc a and 5′-u gag aaa uca cac ucu uaa; si-CHIP, 5′-gga gca ggg caa ucg ucu g and 5′-c aga cga uug ccc ugc ucc; si-BAP1, 5′-cuc cau cag acc aau cca a and 5′-u ugg auu ggu cug aug gag. The siGENOME SMARTpool siRNAs for BAP1 (M-005791-00) and CHIP (M-007201-02) were also used. siRNA transfections were performed using Lipofectamine RNAiMax (Thermo Fisher Scientific, USA) and calcium phosphate methods.

Site-directed mutagenesis

Site-directed mutagenesis was performed with a QuikChange mutagenesis kit and *Pfu* turbo polymerase (Stratagene, USA). The following oligos were used: Ino80-Δ3-1 (R880), 5′-ctc tct ttc aca gaa ggg gta tta atg aag, and 5′-ctt cat taa tac ccc ttc tgt gaa aga gag; Ino80-Δ3-2 (R921), 5′-gct ctt ttc ctg tct ctg agg gcc tcc tac agg ctc c, and 5′-gga gcc tgt agg agg ccc tca gag aca gga aaa gag c; Ino80-Δ6-1 (R1141), 5′-tac atg

gtt tac agg agg cat acc tac atg, and 5′-cat gta ggt atg cct cct gta aac cat gta; Ino80-Δ6-1 (R1152), 5′-gat ggc tca tcc agg atc tcg gag agg, and 5′-cct ctc cga gat cct gga tga gcc atc; Ino80-Δ6-2 (R1217), 5′-tta ggg cag aca agg cag gtt act gtg, and 5′-cac agt aac ctg cct tgt ctg ccc taa; Ino80-Δ6-2 (R1227), 5′-cgg ctc atc tgt aga ggc acc att gaa gaa cgc, and 5′-gcg ttc ttc aat ggt gcc tct aca gat gag ccg; Ino80-Δ6-2 (R1239/1241), 5′-ctg caa aga gcc agg gag agg agt gag att cag, and 5′-ctg aat ctc act cct ctc cct ggc tct ttg cag; CHIP-K30A, 5-gcg cgc agg agc tcg cgg agc agg gca atc g, and 5′-cga ttg ccc tgc tcc gcg agc tcc tgc gcg c; CHIP-H260Q, 5′-gga cat cga gga gca gct gca gcg tgt ggg, and 5′-ccc aca cgc tgc agc tgc tcc tcg atg tcc.

In vivo ubiquitination assay

293T cells were cotransfected with Flag-Ino80 and Ha-Ub vectors along with other expression vectors where indicated for 48 h. After treatment with MG132 at 10 μM for 4 h where indicated, cells were suspended in NETN buffer (20 mM Tris-Cl pH 8.0, 150 mM NaCl, 1 mM EDTA pH 8.0, 0.5% NP-40, 10 mM NaF, and protease inhibitor cocktail containing 0.5 mM phenylmethylsulphonyl fluoride [PMSF], 50 μg/ml pepstatin A, 5 μg/ml leupeptin, and 5 μg/ml aprotinin) and incubated on ice for 30 min. After clarification by centrifugation at 15,000*g* at 4°C for 15 min, lysates were precleared by incubation with protein G Sepharose (16-266; Millipore) at 4°C for 2 h and further incubated with anti-Flag M2 affinity gel (A2220; Sigma) at 4°C overnight. After washing several times with NETN buffer, the beads were suspended in sample loading buffer and boiled for 5 min before being subjected to SDS-PAGE and immunoblotting (IB).

For *in vivo* ubiquitination assays under denaturing conditions, cells were suspended in lysis buffer containing 25 mM Tris-Cl pH 7.5, 1% SDS, 10 mM NaF, and protease inhibitor cocktail (0.5 mM PMSF, 50 μg/ml pepstatin A, 5 μg/ml leupeptin, and 5 μg/ml aprotinin) and incubated at room temperature (RT) for 30 min. Lysates were sonicated at 30% amplitude using a Cole-Parmer Ultrasonic Homogenizer (three times, 10 s each; Cole-Parmer, USA) and clarified by centrifugation at 15,000*g* at 4°C for 15 min. The supernatants were dissolved in EB300 high salt buffer (50 mM Tris-Cl pH7.5, 300 mM NaCl, 1% NP-40, 10 mM β-mercaptoethanol, protease inhibitor cocktail containing 0.5 mM PMSF, 50 μg/ml pepstatin A, 5 μg/ml leupeptin, and 5 μg/ml aprotinin) to dilute SDS concentration to 0.1% and then incubated with primary antibodies and protein G Sepharose at 4°C overnight. After washing several times with EB300 buffer, the beads were suspended in sample loading buffer and boiled for 5 min before being subjected to SDS-PAGE and IB.

Mass spectrometry analysis

Cells were suspended in lysis buffer (2 mM EDTA pH 8.0, 150 mM NaCl, 0.5% sodium deoxycholate, 0.1% SDS, 50 mM Tris-Cl pH 8.0, and 1% NP-40) and incubated on ice for 30 min. After clarification by centrifugation, lysates were precleared by incubation with protein G Sepharose at 4°C for 2 h and incubated with 10 μl of anti-Flag M2 affinity gel at 4°C overnight. After centrifugation, the pellet was washed four times with lysis buffer and suspended in sample loading buffer and boiled for 5 min. Protein samples were run on 7% SDS gel, which was silver stained using a kit (17-1150-01; GE Healthcare, USA). The protein bands of interest were excised and subjected to mass spectrometry analysis using NanoLC-ESI-q-TOF tandem MS.

Immunoprecipitation (IP) and IB

IP was performed as previously described (Lee et al., 2014). In brief, cell lysates in NETN buffer were pre-cleared by incubation with protein G Sepharose and further incubated with primary antibodies and then with protein G Sepharose. After washing with NETN buffer several times, the pellet was suspended in sample loading buffer and boiled before being subjected to SDS-PAGE and IB. For IB for whole cell lysates, cells were suspended in lysis buffer containing 25 mM Tris-Cl pH 7.5, 1% SDS, 10 mM NaF and protease inhibitor cocktail (0.5 mM PMSF, 50 μg/ml pepstatin A, 5 μg/ml leupeptin, and 5 μg/ml aprotinin) and incubated at RT for 30 min. Lysates were then sonicated at 30% amplitude using Branson Sonifier 450 Sonicator (10 s pulses for 2 min, 10 s pause between pulses). Where indicated, cells were suspended in RIPA buffer (50 mM Tris-Cl pH 8.0, 0.1% SDS, 150 mM NaCl, 1% NP-40, and 0.5% deoxycholic acid) and incubated on ice for 30 min. Lysates were dissolved in sample loading buffer and boiled for 5 min.

Proximity ligation assay (PLA)

PLA was performed according to the manufacture's protocol (Sigma). The cells grown on glass cover slides were treated with Leptomycin B (L2913; Sigma) at 20 nM for 1 h where indicated and then fixed with 3.7% paraformaldehyde for 15 min. Samples were washed three times with phosphate-buffered saline (PBS) for 5 min each time, and blocked with 5% bovine serum albumin (BSA) in PBS containing 0.3% Triton X-100 at RT for 1 h. The slides were then incubated with primary antibodies in a humidity chamber at 4°C overnight and blocked in the Duolink blocking buffer at 37°C for 1 h. After washing twice with the Duolink wash buffer A at RT for 5 min each time, the slides were incubated with the PLUS and MINUS PLA probes for 37°C for 1.5 h. The slides were washed twice with the Doulink wash buffer A for 5 min each time and incubated with the Duolink ligation stock at 37°C for 1 h. After washing twice with the wash buffer A for 5 min each time, the slides were incubated with the Duolink polymerase in amplification stock at 37°C for 2 h. The slides were finally washed twice with the Duolink wash buffer B for 5 min each time, counterstained with DAPI for 5 min and mounted using Vectashield mounting medium. Confocal images were captured using a Zeiss LSM 880 microscope (Zeiss, Germany).

Chromatin fractionation

The salt gradient chromatin fractionation was performed as previously described (Park et al., 2020). Briefly, cells were lysed in CEBN buffer (10 mM HEPES [pH 7.8], 10 mM KCl, 1.5 mM $MgCl_2$, 0.34 M sucrose, 10% glycerol, 0.2% NP-40, protease inhibitors as described above) and centrifuged to separate supernatant (cytoplasmic fraction) from pellet. The pellet was suspended in soluble nuclear buffer (3 mM EDTA,

0.2 mM EGTA, protease inhibitors as described above) and centrifuged to separate supernatant (soluble nuclear fraction) from pellet. The resulting pellet was then subjected to gradient salt extraction with salt buffers with increasing NaCl concentration (50 mM Tris [pH 8.0], 0.05% NP-40, NaCl as indicated, protease inhibitors as described above). The one-step detergent fractionation was performed as previously described (Lee et al., 2019; Park et al., 2006). Briefly, 2×10^5 cells were suspended in 100 μl of the fractionation III buffer (50 mM HEPES pH 7.5, 150 mM NaCl, 1 mM EDTA, 0.5% NP-40, protease inhibitor cocktail [0.5 mM PMSF, 50 μg/ml pepstatin A, 5 μg/ml leupeptin, and 5 μg/ml aprotinin], and 10 mM NaF) for 60 min on ice and then centrifuged at 16,000*g* for 20 min to separate supernatant (cytoplasmic and chromatin-unbound or loosely bound proteins) from pellet (insoluble chromatin-bound proteins).

DNA fiber assay

The DNA fiber assay was performed as previously described (Lee et al., 2014; Merrick et al., 2004). Briefly, cells were treated sequentially with IdU for 10 min and CldU for 30 min and then incubated in spreading buffer (0.5% SDS, 200 mM Tris-Cl pH 7.4, and 50 mM EDTA) on a Silane-Prep Slide (S4651; Sigma-Aldrich). DNA fibers were then extended by tilting the slide and were fixed with 3:1 methanol/acetic acid. After treatment with 2.5 N HCl for 30 min, each slide was incubated with mouse anti-BrdU (for IdU detection) and rat anti-BrdU (for CldU detection). After wash with PBS, the slide was incubated with a mixture of secondary antibodies (Alexa Fluor® 568 rabbit anti-mouse IgG [A11061; Invitrogen] and Alexa Fluor®488 chicken anti-rat IgG [A21470; Invitrogen]) at RT for 30 min followed by another mixture of secondary antibodies (Alexa Fluor®568 goat anti-rabbit IgG [A11011; Invitrogen] and Alexa Fluor®488 goat anti-chicken IgG [A11039; Invitrogen]) after 15 min of blocking. The slides were mounted using Vectashield mounting medium and fluorescence microscopy images were captured using a Carl Zeiss LSM880 scanning laser confocal microscope (Fluorescence Core Imaging Center at Ewha Womans University). Tract length of fork progression was determined and converted to fork speed on the basis of 1-μm DNA being equivalent to approximately 2.8 kb.

Statistical analysis

DNA fiber assay was analyzed by Welch's two tailed *t*-test using GraphPad Prism 5.01 (GraphPad Software, USA) and Student's *t*-test using Microsoft Excel 2016 (Microsoft, USA). Data are mean ± SD. *P* values less than 0.05 were considered statistically significant. Uncropped gels are shown in Supplementary Material.

RESULTS

Identification of potential E3 ligase binding sites in Ino80

In an effort to find the E3 ubiquitin ligase for Ino80, we constructed a set of plasmid vectors expressing serial N-terminal deletion mutants of Flag-tagged Ino80 (Fig. 1A) and performed an *in vivo* ubiquitination assay with these constructs. Deletion of the amino acid sequence between positions 851 and 941 greatly reduced Ino80 ubiquitination (Figs. 1B and 1C; compare Δ3 and Δ4). Additional deletion of the sequence between 1121 and 1211, the HelicC domain, almost completely abolished Ino80 ubiquitination (Figs. 1C and 1D; compare Δ6 and Δ7). Thus, these two subregions of Ino80 likely provide either E3 ligase binding sites or ubiquitination sites. We tested the possibility that they provide ubiquitination sites. The N-terminal subregion contains two Lys residues (Fig. 1E), and mutation of these residues to Arg (nonubiquitinatable) either individually or simultaneously (Δ3-1 to Δ3-3) had no effect on Ino80 ubiquitination (Fig. 1F). There are two Lys residues within the HelicC domain and four in its downstream flanking sequence between positions 1211 and 1246 (Fig. 1E). Mutation of these six Lys residues to Arg residues in various combinations (Δ6-1 to Δ6-3) showed no effect on Ino80 ubiquitination (Fig. 1G). Therefore, we concluded that these two subregions of Ino80 provide E3 ligase binding sites rather than ubiquitination sites. We ensured that the expression levels of Flag-Ino80 comparable with those of endogenous Ino80 to prevent possible artifactual effects caused by overexpression of the transfected gene (Supplementary Fig. S1). We note that all the N-terminal deletion mutants of Flag-Ino80 showed higher expression levels with a tendency to degrade compared to full-length Ino80.

CHIP and Hsp70 interact with Ino80

The above results prompted us to identify the cellular proteins that bind to the two subregions of Ino80. In this study, we focused on the HelicC domain. We observed in IP experiments with Flag-Ino80 and its deletion mutants that a group of proteins migrating to approximately 70 kDa were associated with full-length Ino80, Ino80-Δ5 and Ino80-Δ6 but were barely associated with Ino80-Δ7 and Ino80-Δ10 (Fig. 2A), indicating that the HelicC domain was important for their binding to Ino80. These proteins were not general purification contaminant, as they were not present in the vector samples or associated with the chromatin remodeler BRG1 or p53 (Fig. 2A, Supplementary Fig. S2A). Mass spectrometry analysis identified these proteins as Hsp70 and Hsc70, members of the heat shock protein 70 family (Fig. 2B, Supplementary Fig. S2B). Actin-related protein 8 (Arp8), a subunit of the INO80 complex, was also identified to associate with Ino80 (Supplementary Fig. S2B). Using an anti-Hsp70 antibody, we confirmed that Hsp70 binds to Ino80 in a manner dependent on the HelicC domain (Fig. 2C) and is not a purification contaminant (Supplementary Fig. S2C). We further verified the binding of Hsp70 to Ino80 by IP using Myc-tagged Hsp70 (Fig. 2D).

Since CHIP functions as a complex with Hsp70, we performed co-IP to determine whether CHIP interacts with Ino80. When Flag-tagged proteins were immunoprecipitated from cells expressing Flag-Ino80, CHIP and Hsp70 were coprecipitated (Fig. 2E). IP of Flag-tagged proteins from cells expressing Flag-Hsp70 resulted in coprecipitation of Ino80 and CHIP (Fig. 2F). In addition, Ino80 and Hsp70 coprecipitated when Myc-tagged proteins were immunoprecipitated from cells expressing Myc-CHIP (Fig. 2G). These results indicated that both CHIP and Hsp70 were associated with Ino80 within the cells. Consistent with these results, CHIP interacted

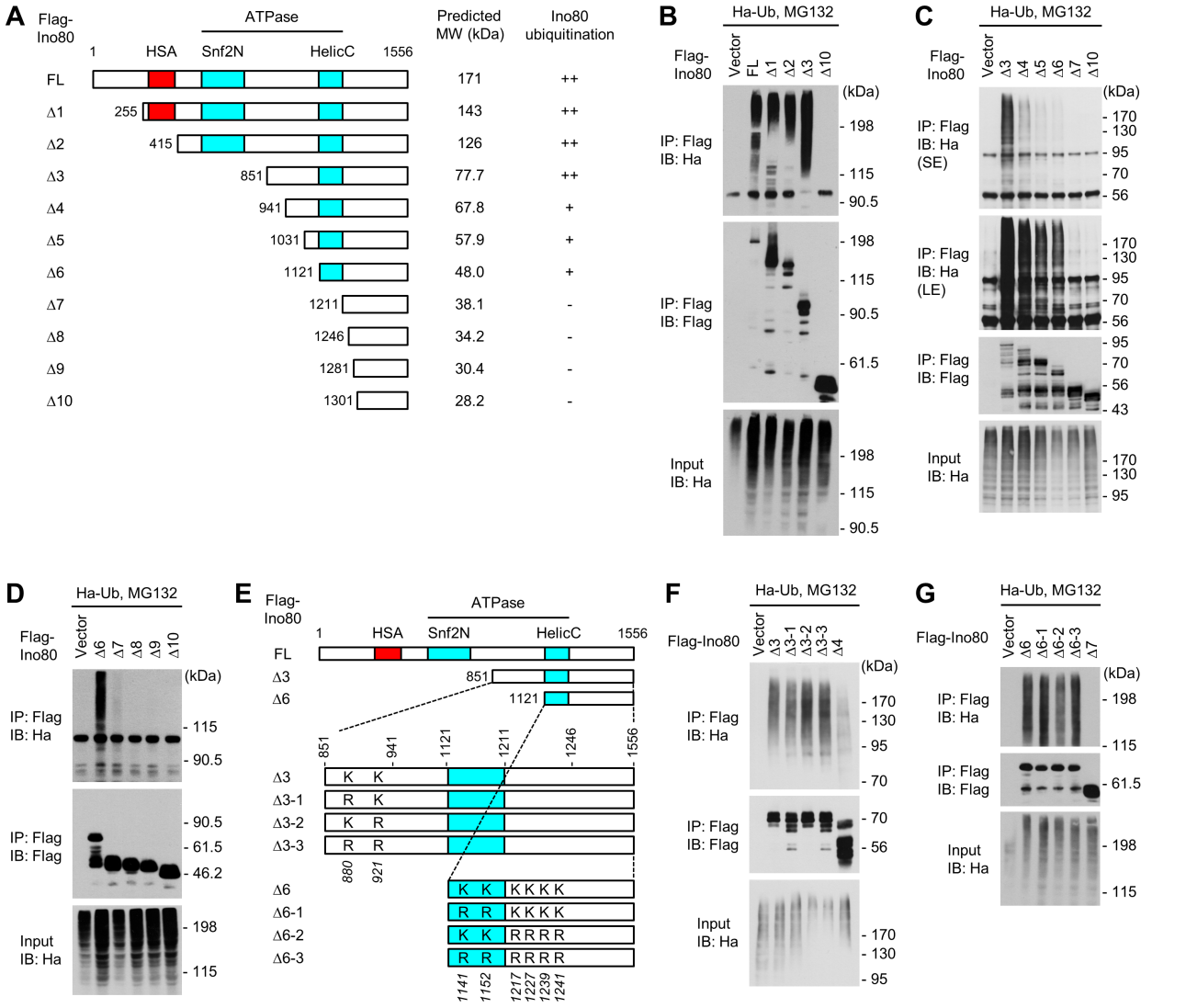

Fig. 1. Identification of potential E3 ligase binding sites in Ino80. (A) Map of the full-length (FL) and serial N-terminal deletion mutants of Flag-tagged Ino80 was shown along with predicted molecular weight (MW) and the relative ubiquitination level for each construct. The ATPase domain of Ino80 splits into the Snf2N and HelicC domains. HSA, helicase-SANT-associated domain; Snf2N, Snf2 family N terminus; HelicC, helicase superfamily C terminus. (B-D) Results of *in vivo* ubiquitination assay for FL and the deletion mutants of Flag-Ino80. A representative of three to five independent experiments showing similar results is presented for each set. SE, short exposure; LE, long exposure. (E) Map of the mutant forms of Ino80-Δ3 and Ino80-Δ6, in each of which the indicated Lys residues were changed to Arg. (F and G) Results of *in vivo* ubiquitination assay for the mutant sets of Flag-Ino80-Δ3 and Flag-Ino80-Δ6. A representative of three independent experiments showing similar results is presented for each set.

with Ino80 in a HelicC domain-dependent manner, similar to Hsp70 (Fig. 2H).

Next, we performed an *in situ* PLA, which not only directly detects protein-protein interactions at the single-molecule level in cells but also allows visualization of the actual intracellular sites of the interactions (Soderberg et al., 2006). Incubation of cells with anti-Ino80 and anti-CHIP antibodies produced clear PLA signals, which were not detected after Ino80 knockdown (Figs. 2I and 2J), demonstrating that Ino80 and CHIP interact directly with each other intracellularly. Similar experiments using anti-Ino80 and anti-Hsp70 antibodies verified the interaction between Ino80 and Hsp70 (Figs. 2I and 2J). Although Ino80 is a nuclear protein, the PLA signals indicated that the interactions of Ino80 with CHIP and Hsp70 occur in both the nucleus and cytoplasm. Interestingly, after treatment of the cells with leptomycin B, a potent nuclear export inhibitor, the majority of the PLA signals were detected in the nucleus (Figs. 2K and 2L). Ino80 may function as a nucleocytoplasmic shuttling protein and this possibility remains to be investigated in future studies.

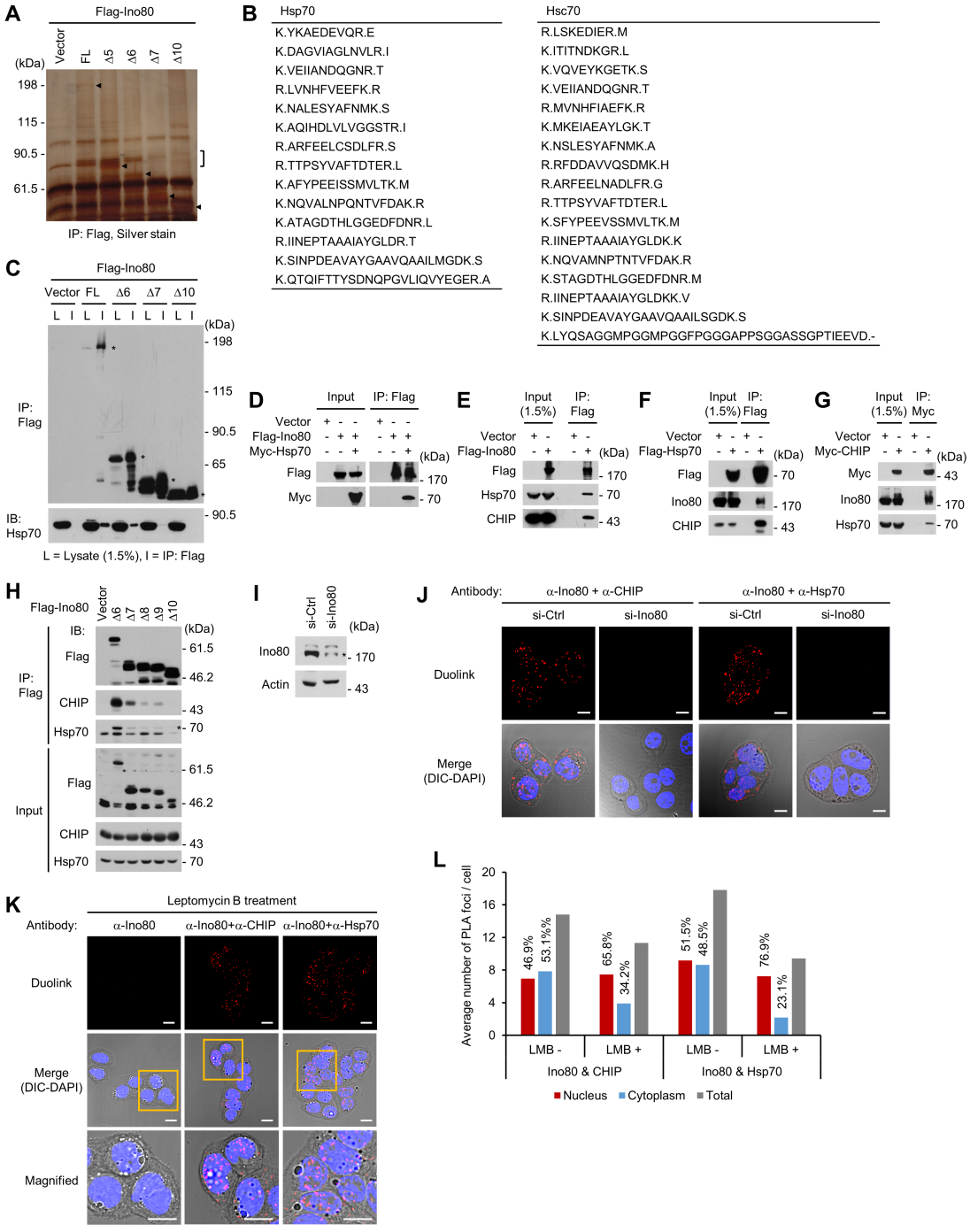

Fig. 2. CHIP and Hsp70 interact with Ino80. (A) After transfection of 293T cells with the indicated expression vectors, Flag-tagged proteins were immunoprecipitated and separated on an SDS gel before silver staining. The bracket indicates the group of proteins that bind to Ino80 dependently of the HelicC domain. Arrowheads, Flag-tagged proteins. FL, full-length. (B) The peptides identified to match Hsp70 and Hsc70 in mass spectrometry analysis. (C) Co-IP results showing the HelicC domain-dependent Hsp70 binding to Ino80. (D) Confirmation of the interaction between Ino80 and Hsp70 by co-IP using Myc-tagged Hsp70. (E-G) Co-IP results demonstrating the interactions among Flag-Ino80, Hsp70, and CHIP (E); Flag-Hsp70, Ino80, and CHIP (F); and Myc-CHIP, Ino80, and Hsp70 (G). (H) Co-IP results showing that both CHIP and Hsp70 bind to Ino80 in a HelicC domain-dependent manner. (I) siRNA knockdown of Ino80 for *in situ* PLA. Asterisk, Ino80 band. (J) Results of the *in situ* PLA demonstrating direct interactions between Ino80 and CHIP and between Ino80 and Hsp70 in HT29 cells. Each spot of red fluorescence represents a single interaction. Ino80 knockdown shows the specificity of the PLA signals. (K) Results of the *in situ* PLA with HT29 cells after leptomycin B treatment (LMB). Scale bars = 10 μm (J and K). (L) The average number of PLA foci in the nucleus and cytoplasm per cell before and after leptomycin B treatment was calculated and depicted as graph. Counted cell number: Ino80/CHIP-LMB, 22; Ino80/CHIP+LMB, 18; Ino80/Hsp70-LMB, 23; Ino80/Hsp70+LMB, 32.

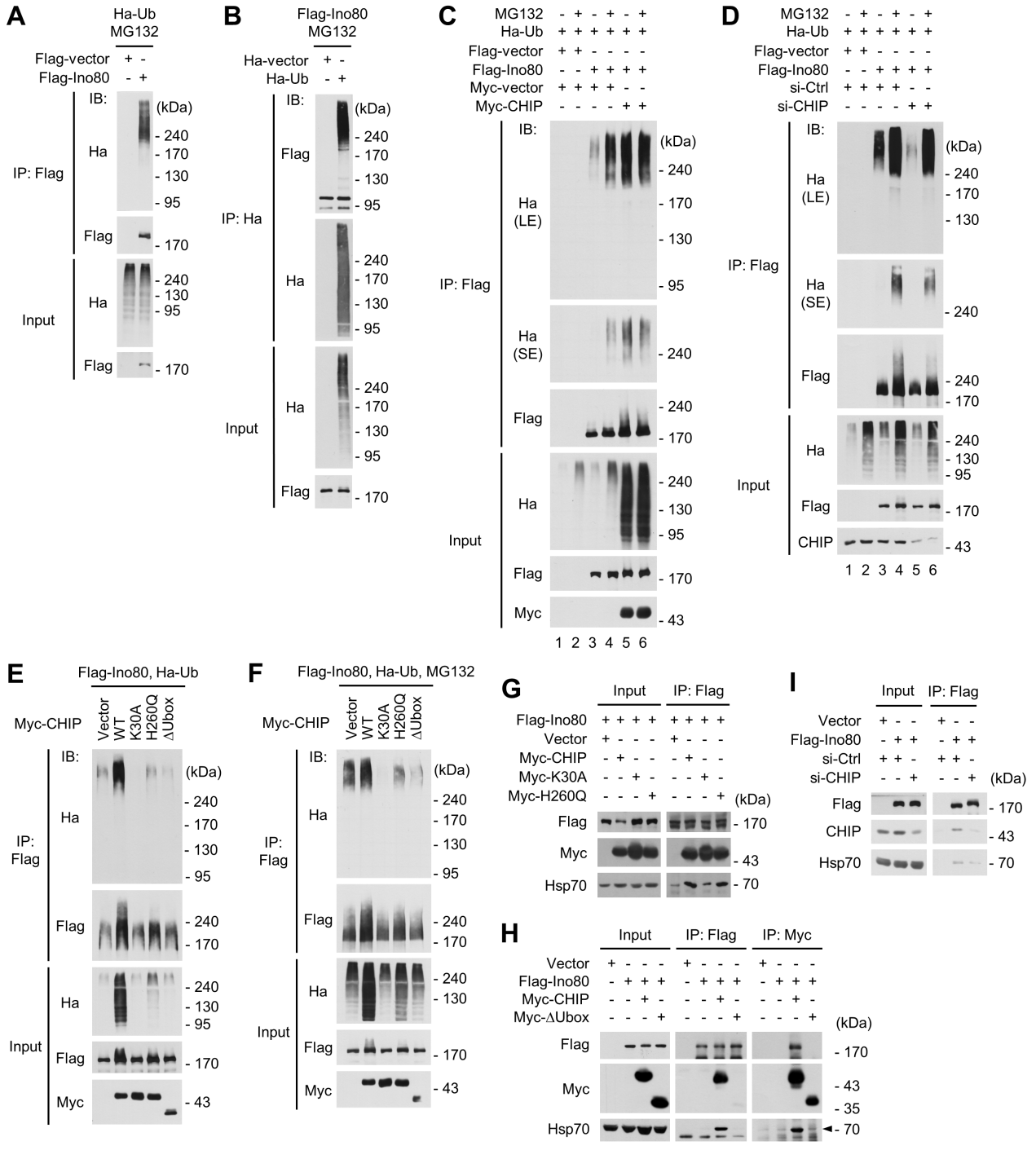

Fig. 3. CHIP polyubiquitinates Ino80 in a manner dependent on Hsp70. (A and B) *In vivo* ubiquitination assay under denaturing condition demonstrates the covalent conjugation of ubiquitin to Ino80. 293T cells were cotransfected with Flag-Ino80 and Ha-Ub vectors and treated with MG132. Flag-tagged (A) and Ha-tagged proteins (B) were immunoprecipitated from cell lysates and analyzed for Ha-Ub and Flag-Ino80 by IB, respectively. (C) After cotransfection with Flag-Ino80 and/or Myc-CHIP plus Ha-Ub, 293T cells were left untreated or treated with MG132 before being subjected to *in vivo* denaturing ubiquitination assay. (D) After cotransfection with Flag-Ino80 and Ha-Ub plus nonspecific or CHIP-specific siRNAs, 293T cells were left untreated or treated with MG132 before being subjected to *in vivo* denaturing ubiquitination assay. LE, long exposure; SE, short exposure. (E and F) After cotransfection with Flag-Ino80 and Ha-Ub plus Myc-CHIP in the forms of wild type or various mutants, 293T cells were left untreated (E) or treated with MG132 before being subjected to *in vivo* denaturing ubiquitination assay (F). (G and H) 293T cells were cotransfected with Flag-Ino80 plus Myc-CHIP in the forms of wild type, K30A, H260Q (G), or ΔUbox mutants (H), and subjected to co-IP and IB. (I) 293T cells were cotransfected with tFlag-Ino80 plus control or CHIP-specific siRNAs, and subjected to co-IP and IB.

CHIP polyubiquitinates Ino80 in a manner dependent on Hsp70

Before pursuing further investigation, we clarified whether the ubiquitination signals detected in our previous assay are attributed to Ino80 or to unrelated, associated proteins since the NETN lysis buffer used in that assay does not completely disrupt noncovalent interaction. After cotransfection with Flag-Ino80 and Ha-tagged ubiquitin (Ha-Ub), cells were treated with MG132 and lysed under denaturing conditions to remove any associated proteins from Flag-Ino80. When Flag-Ino80 was immunoprecipitated, polyubiquitination signals were detected (Fig. 3A). Conversely, in a similar experiment, IP of Ha-Ub resulted in detection of signals representing polyubiquitinated Ino80 (Fig. 3B). The results of these reciprocal denaturing ubiquitination assays demonstrated that Ino80 contains covalently conjugated ubiquitin molecules.

Then, by an *in vivo* ubiquitination assay under denaturing conditions (hereafter, all *in vivo* ubiquitination assays were carried out under denaturing conditions), we determined whether CHIP ubiquitinates Ino80. Ino80 ubiquitination was readily detected under normal conditions (without MG132), and this ubiquitination was increased by MG132 treatment (Fig. 3C, lanes 3 and 4). CHIP overexpression increased Ino80 ubiquitination (Fig. 3C, compares lanes 3 and 4 with lanes 5 and 6), and CHIP knockdown decreased Ino80 ubiquitination independent of MG132 treatment (Fig. 3D, compares lanes 3 and 4 with lanes 5 and 6), showing that CHIP ubiquitinates Ino80 intracellularly. Notably, the effects of CHIP overexpression and knockdown on Ino80 ubiquitination were much more prominent under untreated conditions than under treatment with MG132, apparently due to the increased basal levels of Ino80 in the presence of MG132 (Figs. 3C and 3D).

The U box domain contains the catalytic active site and is essential for CHIP dimerization and substrate binding (Cyr et al., 2002; Jiang et al., 2001). The TPR motif of CHIP mediates its interaction with Hsp70 (Zhang et al., 2005). The catalytic mutant CHIP-H260Q, in which the critical His residue in the active site was changed to Gln, and the CHIP-ΔUbox mutant, which lacks the entire U box, did not increase Ino80 ubiquitination regardless of MG132 treatment (Figs. 3E and 3F), showing that the activity of CHIP towards Ino80 is specific. The CHIP-K30A mutant, which cannot bind to Hsp70 owing to mutation of the critical Lys residue in the TPR motif, was not able to increase Ino80 ubiquitination regardless of MG132 treatment (Figs. 3E and 3F), suggesting that Hsp70 is essential for the Ino80-ubiquitinating activity of CHIP. Both CHIP-H260Q and CHIP-K30A normally bound to Ino80 (Fig. 3G), indicating that neither the catalytic activity nor the Hsp70 binding ability of CHIP is necessary for its binding to Ino80. While CHIP overexpression increased Hsp70 binding to Ino80 (Figs. 3G and 3H), CHIP-ΔUbox was unable to bind to Ino80 and did not increase Hsp70 binding to Ino80 (Fig. 3H). CHIP knockdown decreased Hsp70 binding to Ino80 (Fig. 3I). Therefore, it appears that Hsp70 binds to Ino80 via CHIP and it promotes Ino80 ubiquitination by mechanisms other than mediating the binding of CHIP to Ino80.

CHIP stabilizes Ino80 and most of the CHIP-stabilized Ino80 binds to chromatin

During the course of our study, we repeatedly observed that CHIP overexpression resulted in an increase in Ino80 in the lysates prepared for the denaturing ubiquitination assay, whereas it decreased Ino80 in the lysates prepared for the IP experiment (compare the input lysates in Figs. 3E and 3G, for example), suggesting that the cell lysis conditions could result in this difference. Indeed, the lysis conditions for denaturing ubiquitination (lysis in 1% SDS and sonication) permitted complete extraction of Ino80, whereas the NETN buffer used for IP (data not shown) and the standard RIPA buffer only partially extracted Ino80, resulting in a reduction of Ino80 in the supernatant, with a concomitant increase of Ino80 in the pellet, upon CHIP overexpression (Supplementary Fig. S3). These results suggested that contrary to our expectation that CHIP degrades Ino80, CHIP stabilizes Ino80. Indeed, we observed by using denaturing lysis conditions that increasing CHIP expression resulted in dose-dependent increases in endogenous Ino80 (Fig. 4A) and transfected Flag-Ino80 (Fig. 4E, whole-cell lysate), and inversely, CHIP knockdown decreased both endogenous Ino80 (Fig. 4B) and transfected Flag-Ino80 (Fig. 4C).

Chromatin fractionation with a salt gradient showed that a vast majority of Ino80, even after a large increase in the abundance via CHIP overexpression, was extracted with 0.3- and 0.45-M NaCl, with essentially no protein present in the nuclear unbound fractions, indicating that most of the CHIP-stabilized Ino80 bound to chromatin (Fig. 4D). We confirmed this finding for transfected Flag-Ino80 by the one-step detergent extraction separating chromatin-bound proteins from proteins unbound or loosely bound to chromatin. Flag-Ino80 increased proportionally after expression of increasing amounts of CHIP, and most of the increased Ino80 was present in the chromatin-bound fractions (Fig. 4E), indicating that most CHIP-stabilized Ino80 bound to chromatin. This activity of CHIP was specific, as none of the three CHIP mutants fully promoted Ino80 stabilization and chromatin binding although CHIP-H260Q exhibited some significant effects (Fig. 4F).

Interestingly, MG132 treatment increased Ino80 as previously shown and this effect of MG132 occurred even when CHIP was depleted (Fig. 4G). These results, together with the finding that the decrease in Ino80 ubiquitination mediated by CHIP knockdown was reversed by MG132 (Fig. 3D), suggest that CHIP antagonizes another E3 ligase that triggers proteasomal degradation, possibly by targeting the same sites on Ino80. In support of this hypothesis, while CHIP ubiquitinated Ino80 via Lys-48 and Lys-63 linkages, which typically trigger protein degradation and nondegradative signaling, respectively, neither linkage led to Ino80 degradation, independent of MG132 treatment (Figs. 4H and 4I).

CHIP and BAP1 act in concert to increase Ino80 stability and chromatin binding

Since BAP1 deubiquitinates and stabilizes Ino80 (Lee et al., 2014), we investigated the relationship between CHIP and BAP1 in Ino80 ubiquitination. In the absence of MG132, individual expression of CHIP and BAP1 increased and decreased

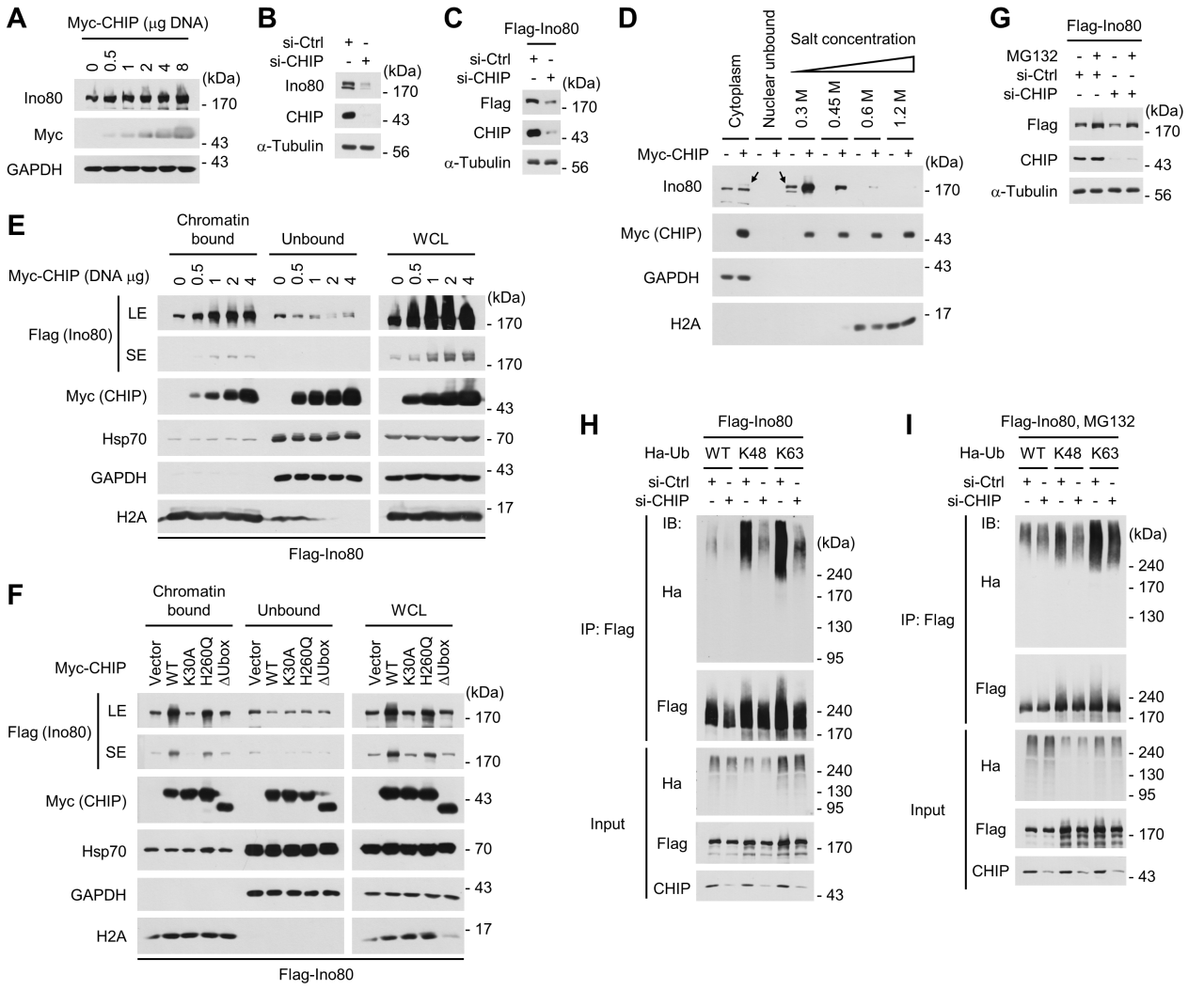

Fig. 4. CHIP stabilizes Ino80, and most of the CHIP-stabilized Ino80 binds to chromatin. (A and B) Immunoblot analysis for 293T cells after transfection with increasing Myc-CHIP expression vector (A) or CHIP-specific siRNAs (B). (C) Immunoblot analysis showing the decrease of Flag-Ino80 by CHIP siRNA knockdown. (D) After transfection with an empty or Myc-CHIP vectors, 293T cells were subjected to salt gradient chromatin fractionation. A representative of two similar results is shown. Arrows, Ino80 band. (E) After cotransfection with Flag-Ino80 and increasing Myc-CHIP, 293T cells were divided into two for the one-step detergent fractionation and for preparation of whole cell lysate (WCL) before being subjected to IB. H2A was used as a marker for insoluble chromatin-bound fraction and GAPDH for soluble unbound fraction. LE, long exposure; SE, short exposure. (F) After cotransfection with Flag-Ino80 plus Myc-CHIP or various mutant Myc-CHIPs, 293T cells were subjected to one-step detergent fractionation as per (E). (G) After cotransfection with Flag-Ino80 plus control or CHIP-specific siRNAs, 293T cells were left untreated or treated with MG132 before immunoblot analysis. (H and I) 293T cells were cotransfected with Flag-Ino80 and Ha-Ub in the forms of wild type, K48 (all Lys residues except Lys-48 mutated to Arg) or K63 mutants (all Lys residues except Lys-63 mutated to Arg), plus control or CHIP-specific siRNAs. Cells were then left untreated (H) or treated with MG132 before being subjected to *in vivo* denaturing ubiquitination assay (I).

Ino80 ubiquitination, respectively, as expected. Notably, compared to expression of CHIP only, coexpression of CHIP with BAP1—but not coexpression with the BAP1(C91S) catalytic mutant—decreased Ino80 ubiquitination, indicating that BAP1 counteracted CHIP-mediated Ino80 ubiquitination (Fig. 5A). Similar experiments in the presence of MG132 showed virtually the same results (Fig. 5B). Expression of increasing amounts of BAP1 diminished CHIP-mediated Ino80 ubiquitination in a dose-dependent manner independent of MG132 treatment (Figs. 5C and 5D), showing the specificity of BAP1 activity. BAP1 overexpression also abolished basal Ino80 ubiquitination (Figs. 5C and 5D, rightmost lanes).

Next, we sought to determine whether CHIP and BAP1 have a combined effect on Ino80 stability. While individual expression of CHIP and BAP1 increased Ino80, as expected, coexpression of these proteins increased endogenous Ino80 (Fig. 5E) and transfected Flag-Ino80 beyond the levels achieved by individual expression of either protein (Fig. 5F).

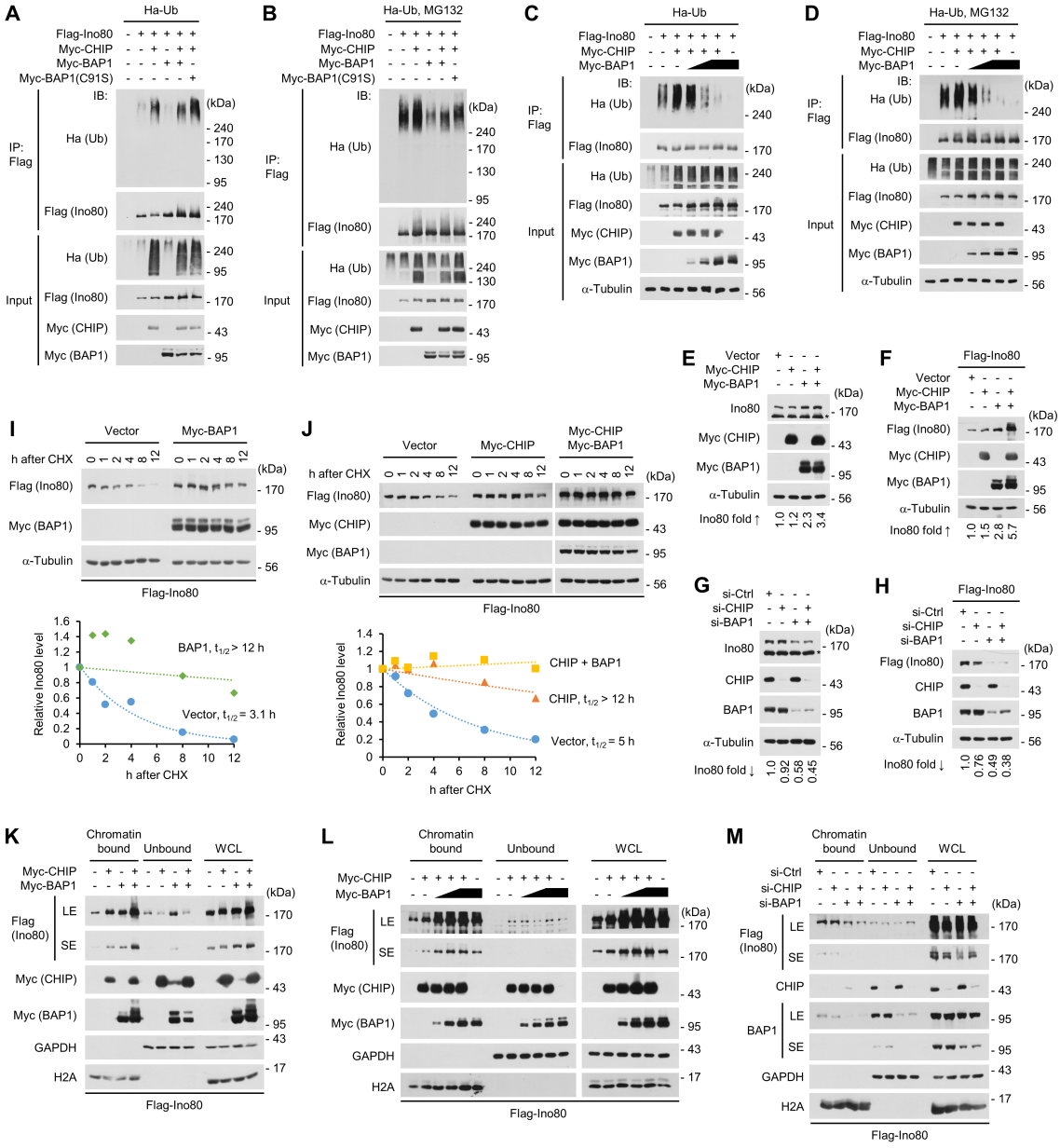

Fig. 5. CHIP and BAP1 act in concert to increase Ino80 stability and chromatin binding. (A and B) BAP1 reduces CHIP-mediated Ino80 ubiquitination. After cotransfection with Flag-Ino80 and Ha-Ub plus Myc-CHIP and/or wild-type or C91S mutant forms of Myc-BAP1, 293T cells were left untreated (A) or treated with MG132 before being subjected to *in vivo* denaturing ubiquitination assay (B). (C and D) BAP1 diminishes CHIP-mediated Ino80 ubiquitination in dose-dependent manner. After cotransfection with Flag-Ino80 and Ha-Ub plus Myc-CHIP and increasing Myc-BAP1, 293T cells were left untreated (C) or treated with MG132 before being subjected to *in vivo* denaturing ubiquitination assay (D). (E) After 293T cells were transfected with Myc-CHIP and/or Myc-BAP1, lysates were prepared for IB. Ino80 fold increase is shown. Asterisk (*), nonspecific band. (F) Results of the similar experiments as in (E) for Flag-Ino80. (G) After 293T cells were transfected with CHIP- and/or BAP1-specific siRNAs, lysates were prepared for IB. Ino80 fold decrease is shown. Asterisk (*), onspecific band. (H) Results of the similar experiments as in (G) for Flag-Ino80. (I and J) (Top) After cotransfection with Flag-Ino80 and Myc-BAP1 (I), or Myc-CHIP or Myc-CHIP plus Myc-BAP1 (J), 293T cells were treated with cycloheximide and harvested at various times for IB. (Bottom) Flag-Ino80 bands were quantitated by densitometer, and after normalization to α-tubulin bands, relative Ino80 levels were plotted as a graph by setting the first lane of each experimental condition as 1. CHX, cycloheximide. (K) After cotransfection with Flag-Ino80 plus Myc-CHIP and/or Myc-BAP1 vectors, 293T cells were subjected to the one-step detergent fractionation as per Fig. 4E. LE, long exposure; SE, short exposure. (L) After cotransfection with Flag-Ino80 plus Myc-CHIP and increasing Myc-BAP1, 293T cells were subjected to the one-step detergent fractionation as per Fig. 4E. (M) After cotransfection with Flag-Ino80 plus CHIP- and/or BAP1-specific siRNAs, 293T cells were subjected to the one-step detergent fractionation as per Fig. 4E.

Conversely, siRNA knockdown of both proteins decreased endogenous Ino80 (Fig. 5G) and transfected Flag-Ino80 below the levels achieved by individual knockdown of either protein (Fig. 5H). Cycloheximide chase assays showed that in the absence of *de novo* protein synthesis, Ino80 decayed with a half-life ranging between 3 h and 5 h, which was extended to longer than 12 h by BAP1 overexpression, as previously shown (Fig. 5I). The Ino80 half-life was also extended to lon-

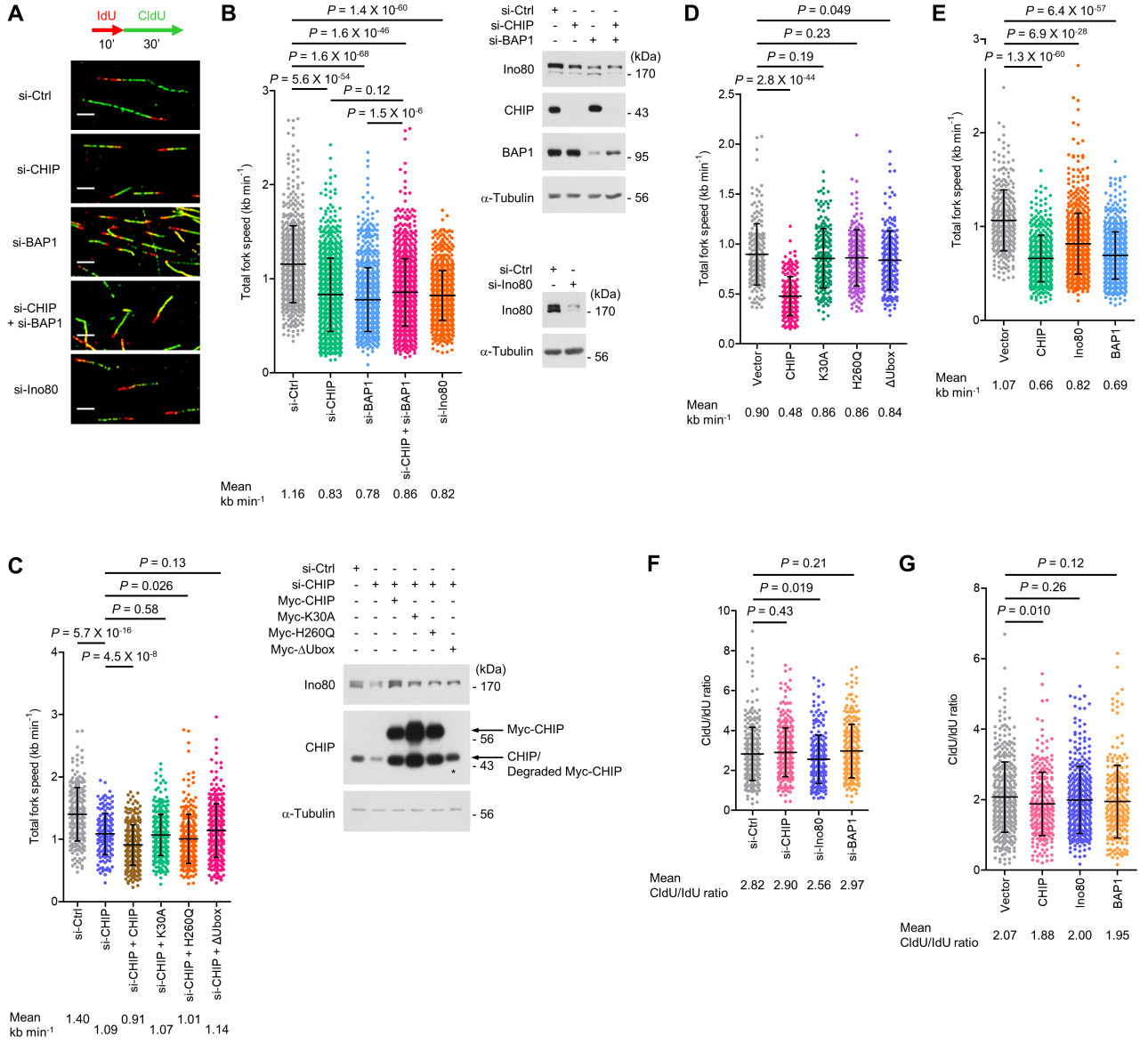

Fig. 6. CHIP and BAP1 work together to regulate replication fork progression. (A-E) After transfection with the expression vectors and/or siRNAs as indicated, 293T cells were subjected to DNA fiber assay. DNA fibers with approximately 2 < CldU/IdU ratio < 4 were counted and depicted as scatter plot. Mean fork speed (kb min^{-1}) is indicated. (A) Representative DNA fibers from the cells transfected with the indicated siRNAs. Scale bars = 5 μm. (B) Scored fibers: si-Ctrl = 613; si-CHIP = 1037; si-BAP1 = 866; si-CHIP + si-BAP1 = 1020; si-Ino80 = 824. The results of immunoblot analysis of siRNA knockdown for DNA fiber assay were shown on the right. (C) Scored fibers: si-Ctrl = 252; si-CHIP = 164; si-CHIP + CHIP = 297; si-CHIP + K30A = 319; si-CHIP + H260Q = 281; si-CHIP + ΔUbox = 324. The results of immunoblot analysis of reexpression of wild-type or various mutants CHIPs in CHIP knockdown cells were shown on the right. Note that degraded Myc-CHIP comigrates with endogenous CHIP. Asterisk (*), Myc-ΔUbox band. (D) Scored fibers: Vector = 200; CHIP = 200; K30A = 200; H260Q = 200; ΔUbox = 200. (E) Scored fibers: Vector = 513; CHIP = 638; Ino80 = 695; BAP1 = 692. (F and G) Using the data from (B) and (E), CldU/IdU ratio was calculated and depicted as scatter plot. Mean CldU/IdU ratios is indicated. (F) Scored fibers: si-Ctrl = 286; si-CHIP = 314; si-Ino80 = 237; si-BAP1 = 245. (G) Scored fibers: Vector = 417; CHIP = 269; Ino80 = 350; BAP1 = 237. Data are mean ± SD. For statistics and reproducibility, see accompanying Supplementary Material (source data).

ger than 12 h by CHIP overexpression, and simultaneous expression of CHIP and BAP1 further increased the half-life (Fig. 5J). Therefore, CHIP, like BAP1, stabilizes Ino80 by prolonging its half-life, and the combined effect of CHIP and BAP1 on Ino80 stabilization is likely attributed to a combination effect on half-life extension.

We then determined the effects of CHIP and BAP1 on chromatin binding of Ino80 by detergent extraction. A majority of the increased amount of Ino80 after simultaneous expression of CHIP and BAP1 bound to chromatin (Fig. 5K). Expression of increasing amounts of BAP1 enhanced CHIP-induced Ino80 stabilization in a dose-dependent manner, with a concomitant increase in chromatin binding of Ino80 (Fig. 5L). Conversely, knockdown of CHIP, BAP1, or both decreased Ino80 preferentially in the chromatin fractions (Fig. 5M). The results obtained thus far collectively suggest that CHIP and BAP1 work together, presumably by promoting nondegradative ubiquitination and removing degradative ubiquitin conjugates, respectively, to augment Ino80 stabilization and chromatin binding. CHIP appears to stabilize Ino80 mainly by inhibiting degradative ubiquitination since BAP1 abolishes both basal and CHIP-mediated ubiquitination and still promotes Ino80 stabilization.

CHIP and BAP1 work together to regulate replication fork progression

Next, we determined the effects of CHIP and BAP1 on replication fork progression by a DNA fiber assay. Individual knockdown of CHIP and BAP1 decreased replication fork progression to an extent similar to the effects achieved by Ino80 knockdown, as evaluated by track length of IdU/CldU incorporation. Simultaneous knockdown of CHIP and BAP1 did not decrease fork progression beyond the levels achieved by individual knockdown of either protein (Figs. 6A and 6B). One reason for this could be that the simultaneous knockdown of CHIP and BAP1 decreased Ino80 only marginally compared to the individual knockdown, which is likely due to a limitation of siRNA knockdown. Contrary to our expectation that reexpression of CHIP would rescue the replication defect in CHIP-depleted cells, CHIP expression instead exacerbated the replication defect in a manner dependent on its catalytic and Hsp70-binding activities (Fig. 6C). Surprisingly, overexpression of CHIP specifically decreased replication fork progression (Fig. 6D). Moreover, overexpression of Ino80 or BAP1 also decreased fork progression (Fig. 6E). Then, we analyzed fork symmetry to determine the effects of CHIP and BAP1 on replication stress. CHIP knockdown showed no effect on fork symmetry (CldU/IdU ratio) (Fig. 6F) and CHIP overexpression reduced it only marginally (Fig. 6G), indicating that the aberrant CHIP levels did not significantly trigger replication stress. Overexpression and knockdown of BAP1 and Ino80 showed little effect on fork symmetry (Figs. 6F and 6G), suggesting that these proteins do not have a significant role in suppressing replication stress during normal DNA synthesis although they are important for stalled fork restart during stress condition (Lee et al., 2019; Vassileva et al., 2014). These results collectively suggest that the stability of Ino80 is critical for DNA replication, meaning that an aberrant level of Ino80, whether deficient or excessive, can compromise fork progression by reducing fork speed rather than by triggering replication stress, and that CHIP, acting together with BAP1, ensures efficient fork progression by optimizing the cellular levels of Ino80.

DISCUSSION

Here, we identified CHIP as an E3 ubiquitin ligase for Ino80 that interacts with, ubiquitinates and stabilizes Ino80 by prolonging its half-life. Our data suggest that CHIP stabilizes Ino80 by inhibiting its degradative ubiquitination. BAP1 abolished both basal and CHIP-mediated Ino80 ubiquitination and still promoted stabilization of Ino80, suggesting that CHIP exerts its Ino80 stabilization activity mostly via inhibition of degradative ubiquitination. Most CHIP- and BAP1-stabilized Ino80 bound to chromatin. Both depletion and overexpression of CHIP compromised replication fork progression with little effect on fork stalling, as observed for BAP1 and Ino80, indicating that an optimal cellular level of Ino80 is important for the speed of replication fork progression but not for suppression of replication stress. These results suggest that CHIP and BAP1 act in concert to regulate Ino80 ubiquitination to fine-tune the stability of Ino80 for efficient DNA replication.

Owing to their ubiquitous expression and important roles in many essential cellular processes, the protein stability of chromatin remodelers were generally thought to be static. However, our previous work showed that the stability of Ino80 is regulated by the ubiquitin-proteasome system and that BAP1 functions as a deubiquitinase that stabilizes Ino80 and thus promotes DNA replication (Lee et al., 2014). In the present work, we aimed to identify the E3 ligase that targets Ino80 for proteasomal degradation and thus functions as an antagonizer of BAP1. Contrary to our expectation, however, CHIP was identified to be an E3 ligase that stabilizes Ino80. Therefore, the Ino80-degrading E3 ubiquitin ligase remains to be discovered. One promising approach to identify this E3 ligase could be to identify the cellular factors that bind Ino80 depending on the subregion between positions 851 and 941. A recent study using co-IP and polyubiquitin affinity pull-down approaches combined with mass spectrometry has identified TRIM3 as a potential E3 ubiquitin ligase for Ino80 functioning in hippocampal synaptic plasticity (Schreiber et al., 2015). Another recent study reported that TRIM3 levels correlate positively with Ino80 polyubiquitination and negatively with Ino80 protein levels during prolonged abstinence from drug exposure (Werner et al., 2019). Thus, it is also worth investigating the possibility that TRIM3 functions as the E3 ubiquitin ligase for Ino80 degradation.

Our data showed that CHIP overexpression leads to a large increase in Ino80 ubiquitination in the absence of MG132, a condition allowing for proteasomal degradation. In addition, CHIP depletion decreased Ino80 ubiquitination, and this effects was reversed by MG132 treatment. Consistent with these results, the decrease in the Ino80 level is reversed by MG132 in CHIP-depleted cells. Based on these results, we propose that CHIP stabilizes Ino80 by competing with the yet-to-be identified Ino80-degrading E3 ligase for ubiquitination, possibly by targeting the same sites. In support of this hypothesis, studies have shown that CHIP ubiquitinates

several proteins via noncanonical ubiquitin linkages, such as K-6 and K-63 linkages, to provide nondegradative signals (McDonough et al., 2009; Ronnebaum et al., 2013; Seo et al., 2018; Yang et al., 2011; Zhu et al., 2014). In this scenario, BAP1 may remove both degradative and CHIP-mediated nondegradative ubiquitin conjugates from Ino80 to ensure maximal protein stability.

As a chaperone-dependent E3 ligase, CHIP works together with Hsp70 or Hsp90 for ubiquitination of its target proteins. Both the K30A mutation and TPR deletion abolish the substrate binding and ubiquitination activities of CHIP towards many target proteins, such as ErbB2, LRRK2, hTERT, Foxp3 and Runx2, showing that CHIP requires chaperones for both substrate binding and its E3 ligase activity towards the substrate (Chen et al., 2013; Ko et al., 2009; Lee et al., 2010; Li et al., 2008; Xu et al., 2002). In contrast, for some targets, such as BACE and E47, CHIP requires chaperones for substrate ubiquitination but not for substrate binding (Huang et al., 2004; Singh and Pati, 2015). Similarly, our results showed that CHIP requires Hsp70 for Ino80 ubiquitination but not for Ino80 binding, thus providing more examples of the differential chaperone requirements of CHIP target proteins for substrate binding and ubiquitination. Therefore, although a chaperone is essential for the E3 ligase activity of CHIP, the role of the chaperone in the binding of CHIP to the substrate is not likely to be absolute but rather to depend on the type of target protein.

Given our results that CHIP and BAP1 regulate the stability of Ino80, it is possible that these regulators play roles in other INO80-mediated processes, such as DNA repair and genome stability. A number of studies have suggested that CHIP functions as a tumor suppressor and as an oncogene by triggering ubiquitin-mediated degradation of several tumor suppressors and oncogenic proteins, including p53, PTEN, c-Myc, ErbB2 and SRC-3 (Ahmed et al., 2012; Esser et al., 2005; Kajiro et al., 2009; Paul et al., 2013; Seo et al., 2019; Xu et al., 2002). Recent studies suggested that INO80 can also function as both a tumor suppressor and tumor promoter, possibly depending on the cancer type as well as genetic background. In this context, one of the mechanisms by which CHIP contributes to tumorigenesis could be through its activity to control the stability of Ino80 in cooperation with BAP1.

Note: Supplementary information is available on the Molecules and Cells website (www.molcells.org).

ACKNOWLEDGMENTS

We thank Chin Ha Chung for providing the Myc-CHIP and Myc-CHIP-ΔUbox expression vectors. This work was supported by grants from the National Research Foundation of Korea (2018R1A2B2007128, 2019R1A5A609964, and 2019R1A6C1010020).

AUTHOR CONTRIBUTIONS

H.R.S., D.J., and S.L. performed experiments. H.S.L., S.A.L., and S.W.K. provided important technical assistance and scientific expertise. All authors contributed to data analysis and interpretation, and manuscript preparation. J.K. conceived and supervised the project, and wrote the manuscript.

CONFLICT OF INTEREST

The authors have no potential conflicts of interest to disclose.

ORCID

Hye-Ran Seo https://orcid.org/0000-0003-3681-1537
Daun Jeong https://orcid.org/0000-0003-0736-5435
Sunmi Lee https://orcid.org/0000-0002-6477-7316
Han-Sae Lee https://orcid.org/0000-0001-5049-9629
Shin-Ai Lee https://orcid.org/0000-0002-2587-8288
Sang Won Kang https://orcid.org/0000-0001-6446-163X
Jongbum Kwon https://orcid.org/0000-0001-6491-6024

REFERENCES

Ahmed, S.F., Deb, S., Paul, I., Chatterjee, A., Mandal, T., Chatterjee, U., and Ghosh, M.K. (2012). The chaperone-assisted E3 ligase C terminus of Hsc70-interacting protein (CHIP) targets PTEN for proteasomal degradation. J. Biol. Chem. *287,* 15996-16006.

Chambers, A.L., Ormerod, G., Durley, S.C., Sing, T.L., Brown, G.W., Kent, N.A., and Downs, J.A. (2012). The INO80 chromatin remodeling complex prevents polyploidy and maintains normal chromatin structure at centromeres. Genes Dev. *26,* 2590-2603.

Chen, Z., Barbi, J., Bu, S., Yang, H.Y., Li, Z., Gao, Y., Jinasena, D., Fu, J., Lin, F., Chen, C., et al. (2013). The ubiquitin ligase Stub1 negatively modulates regulatory T cell suppressive activity by promoting degradation of the transcription factor Foxp3. Immunity *39,* 272-285.

Conaway, R.C. and Conaway, J.W. (2009). The INO80 chromatin remodeling complex in transcription, replication and repair. Trends Biochem. Sci. *34,* 71-77.

Connell, P., Ballinger, C.A., Jiang, J., Wu, Y., Thompson, L.J., Hohfeld, J., and Patterson, C. (2001). The co-chaperone CHIP regulates protein triage decisions mediated by heat-shock proteins. Nat. Cell Biol. *3,* 93-96.

Cyr, D.M., Hohfeld, J., and Patterson, C. (2002). Protein quality control: U-box-containing E3 ubiquitin ligases join the fold. Trends Biochem. Sci. *27,* 368-375.

Downs, J.A., Allard, S., Jobin-Robitaille, O., Javaheri, A., Auger, A., Bouchard, N., Kron, S.J., Jackson, S.P., and Cote, J. (2004). Binding of chromatin-modifying activities to phosphorylated histone H2A at DNA damage sites. Mol. Cell *16,* 979-990.

Esser, C., Scheffner, M., and Hohfeld, J. (2005). The chaperone-associated ubiquitin ligase CHIP is able to target p53 for proteasomal degradation. J. Biol. Chem. *280,* 27443-27448.

Hatakeyama, S., Yada, M., Matsumoto, M., Ishida, N., and Nakayama, K.I. (2001). U box proteins as a new family of ubiquitin-protein ligases. J. Biol. Chem. *276,* 33111-33120.

Hohfeld, J., Cyr, D.M., and Patterson, C. (2001). From the cradle to the grave: molecular chaperones that may choose between folding and degradation. EMBO Rep. *2,* 885-890.

Hu, J., Liu, J., Chen, A., Lyu, J., Ai, G., Zeng, Q., Sun, Y., Chen, C., Wang, J., Qiu, J., et al. (2016). Ino80 promotes cervical cancer tumorigenesis by activating Nanog expression. Oncotarget *7,* 72250-72262.

Huang, Z., Nie, L., Xu, M., and Sun, X.H. (2004). Notch-induced E2A degradation requires CHIP and Hsc70 as novel facilitators of ubiquitination. Mol. Cell. Biol. *24,* 8951-8962.

Hur, S.K., Park, E.J., Han, J.E., Kim, Y.A., Kim, J.D., Kang, D., and Kwon, J. (2010). Roles of human INO80 chromatin remodeling enzyme in DNA replication and chromosome segregation suppress genome instability. Cell. Mol. Life Sci. *67,* 2283-2296.

Jiang, J., Ballinger, C.A., Wu, Y., Dai, Q., Cyr, D.M., Hohfeld, J., and Patterson, C. (2001). CHIP is a U-box-dependent E3 ubiquitin ligase: identification of Hsc70 as a target for ubiquitylation. J. Biol. Chem. *276,* 42938-42944.

Jin, J., Cai, Y., Yao, T., Gottschalk, A.J., Florens, L., Swanson, S.K., Gutierrez, J.L., Coleman, M.K., Workman, J.L., Mushegian, A., et al. (2005). A mammalian chromatin remodeling complex with similarities to the yeast INO80 complex. J. Biol. Chem. *280,* 41207-41212.

Kajiro, M., Hirota, R., Nakajima, Y., Kawanowa, K., So-ma, K., Ito, I., Yamaguchi, Y., Ohie, S.H., Kobayashi, Y., Seino, Y., et al. (2009). The ubiquitin ligase CHIP acts as an upstream regulator of oncogenic pathways. Nat. Cell Biol. *11,* 312-319.

Ko, H.S., Bailey, R., Smith, W.W., Liu, Z., Shin, J.H., Lee, Y.I., Zhang, Y.J., Jiang, H., Ross, C.A., Moore, D.J., et al. (2009). CHIP regulates leucine-rich repeat kinase-2 ubiquitination, degradation, and toxicity. Proc. Natl. Acad. Sci. U. S. A. *106,* 2897-2902.

Lee, H.S., Lee, S.A., Hur, S.K., Seo, J.W., and Kwon, J. (2014). Stabilization and targeting of INO80 to replication forks by BAP1 during normal DNA synthesis. Nat. Commun. *5,* 5128.

Lee, H.S., Seo, H.R., Lee, S.A., Choi, S., Kang, D., and Kwon, J. (2019). BAP1 promotes stalled fork restart and cell survival via INO80 in response to replication stress. Biochem. J. *476,* 3053-3066.

Lee, J.H., Khadka, P., Baek, S.H., and Chung, I.K. (2010). CHIP promotes human telomerase reverse transcriptase degradation and negatively regulates telomerase activity. J. Biol. Chem. *285,* 42033-42045.

Lee, S.A., Lee, H.S., Hur, S.K., Kang, S.W., Oh, G.T., Lee, D., and Kwon, J. (2017). INO80 haploinsufficiency inhibits colon cancer tumorigenesis via replication stress-induced apoptosis. Oncotarget *8,* 115041-115053.

Li, X., Huang, M., Zheng, H., Wang, Y., Ren, F., Shang, Y., Zhai, Y., Irwin, D.M., Shi, Y., Chen, D., et al. (2008). CHIP promotes Runx2 degradation and negatively regulates osteoblast differentiation. J. Cell. Biol. *181,* 959-972.

McDonough, H., Charles, P.C., Hilliard, E.G., Qian, S.B., Min, J.N., Portbury, A., Cyr, D.M., and Patterson, C. (2009). Stress-dependent Daxx-CHIP interaction suppresses the p53 apoptotic program. J. Biol. Chem. *284,* 20649-20659.

Measday, V., Baetz, K., Guzzo, J., Yuen, K., Kwok, T., Sheikh, B., Ding, H., Ueta, R., Hoac, T., Cheng, B., et al. (2005). Systematic yeast synthetic lethal and synthetic dosage lethal screens identify genes required for chromosome segregation. Proc. Natl. Acad. Sci. U. S. A. *102,* 13956-13961.

Merrick, C.J., Jackson, D., and Diffley, J.F. (2004). Visualization of altered replication dynamics after DNA damage in human cells. J. Biol. Chem. *279,* 20067-20075.

Min, J.N., Tian, Y., Xiao, Y., Wu, L., Li, L., and Chang, S. (2013). The mINO80 chromatin remodeling complex is required for efficient telomere replication and maintenance of genome stability. Cell Res. *23,* 1396-1413.

Morrison, A.J., Highland, J., Krogan, N.J., Arbel-Eden, A., Greenblatt, J.F., Haber, J.E., and Shen, X. (2004). INO80 and gamma-H2AX interaction links ATP-dependent chromatin remodeling to DNA damage repair. Cell *119,* 767-775.

Morrison, A.J., Kim, J.A., Person, M.D., Highland, J., Xiao, J., Wehr, T.S., Hensley, S., Bao, Y., Shen, J., Collins, S.R., et al. (2007). Mec1/Tel1 phosphorylation of the INO80 chromatin remodeling complex influences DNA damage checkpoint responses. Cell *130,* 499-511.

Morrison, A.J. and Shen, X. (2009). Chromatin remodelling beyond transcription: the INO80 and SWR1 complexes. Nat. Rev. Mol. Cell Biol. *10,* 373-384.

Murata, S., Minami, Y., Minami, M., Chiba, T., and Tanaka, K. (2001). CHIP is a chaperone-dependent E3 ligase that ubiquitylates unfolded protein. EMBO Rep. *2,* 1133-1138.

Ogiwara, H., Ui, A., Kawashima, S., Kugou, K., Onoda, F., Iwahashi, H., Harata, M., Ohta, K., Enomoto, T., and Seki, M. (2007). Actin-related protein Arp4 functions in kinetochore assembly. Nucleic Acids Res. *35,* 3109-3117.

Oh, K.H., Yang, S.W., Park, J.M., Seol, J.H., Iemura, S., Natsume, T., Murata, S., Tanaka, K., Jeon, Y.J., and Chung, C.H. (2011). Control of AIF-mediated cell death by antagonistic functions of CHIP ubiquitin E3 ligase and USP2 deubiquitinating enzyme. Cell Death Differ. *18,* 1326-1336.

Papamichos-Chronakis, M., Krebs, J.E., and Peterson, C.L. (2006). Interplay between Ino80 and Swr1 chromatin remodeling enzymes regulates cell cycle checkpoint adaptation in response to DNA damage. Genes Dev. *20,* 2437-2449.

Papamichos-Chronakis, M. and Peterson, C.L. (2008). The Ino80 chromatin-remodeling enzyme regulates replisome function and stability. Nat. Struct. Mol. Biol. *15,* 338-345.

Papamichos-Chronakis, M., Watanabe, S., Rando, O.J., and Peterson, C.L. (2011). Global regulation of H2A.Z localization by the INO80 chromatin-remodeling enzyme is essential for genome integrity. Cell *144,* 200-213.

Park, E.J., Hur, S.K., and Kwon, J. (2010). Human INO80 chromatin-remodelling complex contributes to DNA double-strand break repair via the expression of Rad54B and XRCC3 genes. Biochem. J. *431,* 179-187.

Park, E.J., Hur, S.K., Lee, H.S., Lee, S.A., and Kwon, J. (2011). The human Ino80 binds to microtubule via the E-hook of tubulin: implications for the role in spindle assembly. Biochem. Biophys. Res. Commun. *416,* 416-420.

Park, J.H., Park, E.J., Lee, H.S., Kim, S.J., Hur, S.K., Imbalzano, A.N., and Kwon, J. (2006). Mammalian SWI/SNF complexes facilitate DNA double-strand break repair by promoting gamma-H2AX induction. EMBO J. *25,* 3986-3997.

Park, S.G., Lee, D., Seo, H.R., Lee, S.A., and Kwon, J. (2020). Cytotoxic activity of bromodomain inhibitor NVS-CECR2-1 on human cancer cells. Sci. Rep. *10,* 16330.

Paul, I., Ahmed, S.F., Bhowmik, A., Deb, S., and Ghosh, M.K. (2013). The ubiquitin ligase CHIP regulates c-Myc stability and transcriptional activity. Oncogene *32,* 1284-1295.

Ronnebaum, S.M., Wu, Y., McDonough, H., and Patterson, C. (2013). The ubiquitin ligase CHIP prevents SirT6 degradation through noncanonical ubiquitination. Mol. Cell. Biol. *33,* 4461-4472.

Schreiber, J., Vegh, M.J., Dawitz, J., Kroon, T., Loos, M., Labonte, D., Li, K.W., Van Nierop, P., Van Diepen, M.T., De Zeeuw, C.I., et al. (2015). Ubiquitin ligase TRIM3 controls hippocampal plasticity and learning by regulating synaptic gamma-actin levels. J. Cell Biol. *211,* 569-586.

Seo, J., Han, S.Y., Seong, D., Han, H.J., and Song, J. (2019). Multifaceted C-terminus of HSP70-interacting protein regulates tumorigenesis via protein quality control. Arch. Pharm. Res. *42,* 63-75.

Seo, J., Lee, E.W., Shin, J., Seong, D., Nam, Y.W., Jeong, M., Lee, S.H., Lee, C., and Song, J. (2018). K6 linked polyubiquitylation of FADD by CHIP prevents death inducing signaling complex formation suppressing cell death. Oncogene *37,* 4994-5006.

Shen, X., Mizuguchi, G., Hamiche, A., and Wu, C. (2000). A chromatin remodelling complex involved in transcription and DNA processing. Nature *406,* 541-544.

Shen, X., Xiao, H., Ranallo, R., Wu, W.H., and Wu, C. (2003). Modulation of ATP-dependent chromatin-remodeling complexes by inositol polyphosphates. Science *299,* 112-114.

Shimada, K., Oma, Y., Schleker, T., Kugou, K., Ohta, K., Harata, M., and Gasser, S.M. (2008). Ino80 chromatin remodeling complex promotes recovery of stalled replication forks. Curr. Biol. *18,* 566-575.

Singh, A.K. and Pati, U. (2015). CHIP stabilizes amyloid precursor protein via proteasomal degradation and p53-mediated trans-repression of beta-secretase. Aging Cell *14,* 595-604.

Soderberg, O., Gullberg, M., Jarvius, M., Ridderstrale, K., Leuchowius, K.J., Jarvius, J., Wester, K., Hydbring, P., Bahram, F., Larsson, L.G., et al. (2006). Direct observation of individual endogenous protein complexes in situ by proximity ligation. Nat. Methods *3,* 995-1000.

Tsukuda, T., Fleming, A.B., Nickoloff, J.A., and Osley, M.A. (2005). Chromatin remodelling at a DNA double-strand break site in Saccharomyces cerevisiae. Nature *438,* 379-383.

Vassileva, I., Yanakieva, I., Peycheva, M., Gospodinov, A., and Anachkova, B.

(2014). The mammalian INO80 chromatin remodeling complex is required for replication stress recovery. Nucleic Acids Res. *42,* 9074-9086.

Vincent, J.A., Kwong, T.J., and Tsukiyama, T. (2008). ATP-dependent chromatin remodeling shapes the DNA replication landscape. Nat. Struct. Mol. Biol. *15,* 477-484.

Wang, T., Wang, W., Wang, Q., Xie, R., Landay, A., and Chen, D. (2020). The E3 ubiquitin ligase CHIP in normal cell function and in disease conditions. Ann. N. Y. Acad. Sci. *1460,* 3-10.

Werner, C.T., Mitra, S., Martin, J.A., Stewart, A.F., Lepack, A.E., Ramakrishnan, A., Gobira, P.H., Wang, Z.J., Neve, R.L., Gancarz, A.M., et al. (2019). Ubiquitin-proteasomal regulation of chromatin remodeler INO80 in the nucleus accumbens mediates persistent cocaine craving. Sci. Adv. *5,* eaay0351.

Wu, S., Shi, Y., Mulligan, P., Gay, F., Landry, J., Liu, H., Lu, J., Qi, H.H., Wang, W., Nickoloff, J.A., et al. (2007). A YY1-INO80 complex regulates genomic stability through homologous recombination-based repair. Nat. Struct. Mol. Biol. *14,* 1165-1172.

Xu, W., Marcu, M., Yuan, X., Mimnaugh, E., Patterson, C., and Neckers, L. (2002). Chaperone-dependent E3 ubiquitin ligase CHIP mediates a degradative pathway for c-ErbB2/Neu. Proc. Natl. Acad. Sci. U. S. A. *99,* 12847-12852.

Yang, M., Wang, C., Zhu, X., Tang, S., Shi, L., Cao, X., and Chen, T. (2011). E3 ubiquitin ligase CHIP facilitates Toll-like receptor signaling by recruiting and polyubiquitinating Src and atypical PKC{zeta}. J. Exp. Med. *208,* 2099-2112.

Yu, E.Y., Steinberg-Neifach, O., Dandjinou, A.T., Kang, F., Morrison, A.J., Shen, X., and Lue, N.F. (2007). Regulation of telomere structure and functions by subunits of the INO80 chromatin remodeling complex. Mol. Cell. Biol. *27,* 5639-5649.

Zhang, M., Windheim, M., Roe, S.M., Peggie, M., Cohen, P., Prodromou, C., and Pearl, L.H. (2005). Chaperoned ubiquitylation--crystal structures of the CHIP U box E3 ubiquitin ligase and a CHIP-Ubc13-Uev1a complex. Mol. Cell *20,* 525-538.

Zhang, S., Zhou, B., Wang, L., Li, P., Bennett, B.D., Snyder, R., Garantziotis, S., Fargo, D.C., Cox, A.D., Chen, L., et al. (2017). INO80 is required for oncogenic transcription and tumor growth in non-small cell lung cancer. Oncogene *36,* 1430-1439.

Zhou, B., Wang, L., Zhang, S., Bennett, B.D., He, F., Zhang, Y., Xiong, C., Han, L., Diao, L., Li, P., et al. (2016). INO80 governs superenhancer-mediated oncogenic transcription and tumor growth in melanoma. Genes Dev. *30,* 1440-1453.

Zhu, X., Zhang, J., Sun, H., Jiang, C., Dong, Y., Shan, Q., Su, S., Xie, Y., Xu, N., Lou, X., et al. (2014). Ubiquitination of inositol-requiring enzyme 1 (IRE1) by the E3 ligase CHIP mediates the IRE1/TRAF2/JNK pathway. J. Biol. Chem. *289,* 30567-30577.